

Article

Synergistic Effect of Combined Treatment with Magnetic Hyperthermia and Magneto-Mechanical Stress of Breast Cancer Cells

Rumiana Tzoneva^{1,*}, Aikaterini-Rafailia Tsiapla^{2,3,*}, Veselina Uzunova¹, Tihomira Stoyanova¹, Theodoros Samaras^{2,3}, Makis Angelakeris^{2,3} and Orestis Kalogirou^{2,3}

- ¹ Institute of Biophysics and Biomedical Engineering, Bulgarian Academy of Sciences, Acad. G. Bonchev Str., Bl. 21, 1113 Sofia, Bulgaria
- ² Faculty of Sciences, School of Physics, Aristotle University, 54124 Thessaloniki, Greece
- ³ Center for Interdisciplinary Research and Innovation (CIRI-AUTH), Magna Charta, 57001 Thessaloniki, Greece
- * Correspondence: tzoneva@bio21.bas.bg (R.T.); aitsiapl@physics.auth.gr (A.-R.T.)

Abstract: With the development of nanotechnology, the emergence of new anti-tumor techniques using nanoparticles such as magnetic hyperthermia and magneto-mechanical activation have been the subject of much attention and study in recent years, as anticancer tools. Therefore, the purpose of the current in vitro study was to investigate the cumulative effect of a combination of these two techniques, using magnetic nanoparticles against breast cancer cells. After 24 h of incubation, human breast cancer (MCF-7) and non-cancerous (MCF-10A) cells with and without MNPs were treated (a) for 15 min with magnetic hyperthermia, (b) for 30 min with magneto-mechanical activation, and (c) by a successive treatment consisting of a 15-min magnetic hyperthermia cycle and 30 min of magneto-mechanical activation. The influence of treatments on cell survival and morphology was studied by MTT (3-(4,5-dimethylthiazol-2-yl)-2,5-diphenyltetrazoliumbromide) assay and light microscopy. When applied, separately, magneto-mechanical and thermal (hyperthermia) treatment did not demonstrate strong reduction in cell viability. No morphological changes were observed in non-cancerous cells after treatments. On the other hand, the combination of magneto-mechanical and thermal treatment in the presence of MNPs had a synergistic effect on decreased cell viability, and apoptosis was demonstrated in the cancer cell line. Synergism is most evident in the cancer cell line, incubated for 120 h, while in the non-cancerous line after 120 h, an increase in proliferation is clearly observed. MCF-7 cells showed more rounded cell morphology, especially after 120 h of combined treatment.

Keywords: magnetic hyperthermia; magneto-mechanical activation; magnetic nanoparticles; breast cancer cells; cytotoxicity; apoptosis



Citation: Tzoneva, R.; Tsiapla, A.-R.; Uzunova, V.; Stoyanova, T.; Samaras, T.; Angelakeris, M.; Kalogirou, O. Synergistic Effect of Combined Treatment with Magnetic Hyperthermia and Magneto-Mechanical Stress of Breast Cancer Cells. *Magnetochemistry* **2022**, *8*, 117. <https://doi.org/10.3390/magnetochemistry8100117>

Academic Editor: Joan-Josep Suñol

Received: 24 August 2022

Accepted: 26 September 2022

Published: 29 September 2022

Publisher's Note: MDPI stays neutral with regard to jurisdictional claims in published maps and institutional affiliations.



Copyright: © 2022 by the authors. Licensee MDPI, Basel, Switzerland. This article is an open access article distributed under the terms and conditions of the Creative Commons Attribution (CC BY) license (<https://creativecommons.org/licenses/by/4.0/>).

1. Introduction

In an effort to conquer cancer, many strategies are being used nowadays. Many studies have focused on the development of new anticancer drugs, with the aim of minimizing the damage to healthy tissues and therefore fewer side effects; however, most of them have failed in in vivo and clinical trials [1,2]. Therefore, the need to discover new techniques and methods is imperative. With the development of nanotechnology, the emergence of new anti-tumor techniques, such as magnetic hyperthermia (MHT) became possible. MHT is a technique, where an external alternating magnetic field is used to heat the area of the cancer tissue up to 41–45 °C, due to the local heating of the magnetic nanoparticles (MNPs), which finally leads to cell apoptosis [3]. By taking advantage of differences in the thermal resistance of normal and tumor cells, MHT can kill tumor cells selectively [4]. MHT has been proposed since the 1950s, as a method of treating cancer, using magnetic

implants as thermo-seeds, which, when exposed to an alternating magnetic field (AMF), generate heat. Later, Gordon et al. [5] introduced the concept of “intracellular” MHT, where they used magnetite particles coated with dextran, which were totally internalized in cancer cells in vivo, in order to raise the tumors’ temperature after applying strong AMF. Recently, nanotechnology has contributed, not only to the treatment of cancer but also to its early diagnosis and detection [6]. The most commonly used materials for MHT are nanometer-sized (10–100 nm) ferrite nanoparticles, in particular magnetite (Fe_3O_4) and/or maghemite ($\gamma\text{-Fe}_2\text{O}_3$) [7]. When nanoparticles are exposed to an alternating magnetic field, they produce heat via two main mechanisms: (1) hysteresis loss and (2) relaxational losses [8]. An increase in the local temperature (values between 40 and 44 °C) is sufficient to negatively impact cancer growth [9]. Among the cellular effects upon treatment with MHT are decreased cell viability; cytoskeleton damage; the elevation of oxidative stress; cell cycle arrest; and cellular death by apoptosis [10]. After success in various pre-clinical models, MHT has already entered clinical trials by the direct injection of magnetic nanoparticles into solid tumors such as glioblastoma [11] and prostate carcinoma [12].

A relatively new technique that has increasingly emerged in recent years and is gaining ground towards cancer treatment is magneto-mechanical stress (MM). In this technique, the magnetic field exerts magnetic forces on the MNPs, which in turn applies mechanical forces on malignant and non-malignant cell membranes, causing damage preferentially to cancerous tissues [13–15]. In addition, when MNPs are internalized in the presence of an alternating magnetic field, they can cause mechanical disruption of lysosomes, the release of lysosomal contents, and finally cell death [16,17]. In our previous studies, we showed that application a magneto-mechanical stress (especially pulsed field mode) in combination with MNPs caused the internalization of MNPs, decreased viability, and actin stress fiber alterations and apoptotic changes in MCF-7 and MDA-MB-231 cancer cell lines [18,19].

The concept of multi-functional therapy in cancer has been discussed by many authors. By the combination of different types of therapies, however, the therapeutic index of the treatments can be improved by having non-additive normal tissue side effects but additive or synergistic therapeutic effects [20]. For instance, MHT, in combination with chemotherapy and radiotherapy, has been employed for the treatment of one of the most aggressive tumors—glioblastoma [21,22].

Therefore, the aim of this study will be achieved by the application of a combined strategy using both of the abovementioned techniques: magnetic hyperthermia and magneto-mechanical activation, to achieve an improved anti-cancer effect.

2. Materials and Methods

2.1. Chemicals

The magnetic nanoparticles used in this work were supplied by Chemicell GmbH, Germany (fluid MAG-D, Art No 4101). Fluid MAG-D nanoparticles consist of aqueous dispersions of magnetic iron oxides with an average hydrodynamic diameter of 200 nm and a multi-domain core. Their iron oxide core is covered with a hydrophilic polymer matrix (starch) to protect them against aggregation by foreign ions. All consumables used for cell cultivation have been described previously [18]. Transmission electron microscopy (TEM) and vibrating-sample magnetometer (VSM) measurements of these commercial MNPs have already been published [19,23], confirming the spherical shape of the MNPs, while hysteresis loops at low (5 K) and high temperature (300 K) yielded a distinct saturation magnetization M_s (5K) = 50 and M_s (300K) = 40 Am^2/kg .

2.2. Cell Lines and Cultivation Conditions

Briefly, cancerous MCF-7 (ATCC, HTB-22) and non-cancerous MCF-10A (ATCC, CRL-10317) cell lines were cultivated up to 3×10^5 cells per petri dish (\varnothing 35 mm) in high-glucose (4500 mg/L) DMEM or DMEM F-12 media containing 10% FBS, 1 mM L-Glutamine, penicillin-streptomycin-amphotericin B, sodium pyruvate, non-essential amino acids, and insulin. DMEM F-12 medium for the MCF-10A cell line was supplemented with the addi-

tion of hydrocortisone (50 µg/mL stock solution, Merck, Germany) and human epidermal growth factor (20 ng/mL stock solution, Merck, Germany). Cultivation conditions of cells were 37 °C, 5% CO₂, 95% air, and humid atmosphere.

2.3. Magnetic Hyperthermia (MHT) Set-Up and Treatment

Cancerous MCF-7 and non-cancerous MCF-10A cells were seeded in 35 mm petri dishes in a complete cellular medium containing 100 µg/mL MNPs (when mentioned) and were incubated for 24 h. The above concentration of MNPs proved to non-toxic for the cells in our previous study [24]. Then, the cells were detached and treated with MHT for 15 min until they reached the hyperthermia window (preferably 41–45 °C). Magnetic particle hyperthermia experiments in a commercial AMF generator (1.2 kW Ambrell Easyheat 0112), under a magnetic field amplitude of 60 mT and a frequency of 375 kHz, were performed. Each sample temperature was recorded in 0.4 s intervals for an ample period of time (i.e., 900 s) with an optic fiber temperature sensor immersed in the central region of each sample. It should be mentioned that each measurement consists of a heating part (~up to 900 s), where the temperature increases under the application of an AC magnetic field, and a subsequent cooling part (from 900 s to 1100–1600 s) in the absence of AC field is turned off. The schematic representation of a typical MHT set-up and a typical hyperthermia measurement cycle has been previously published in the Supporting Information of [25].

2.4. Magneto-Mechanical (MM) Set-Up and Treatment

Cell culture dishes containing the aforementioned cells and MNPs (when mentioned) were placed on a novel custom-made MM device with a 3D-printed turntable composed of an array of permanent magnets [13] and then were exposed to a pulsed field mode in extremely low frequency magnetic fields with intensity of 200 mT and frequency of 2 Hz, for a period of 30 min at room temperature.

2.5. Combined Treatment of Cells with MHT and MM

For the combined treatment, cells containing MNPs (when mentioned) were first exposed for 15 min in MHT, as was explained above, and then were exposed for 30 min in MM activation.

For all types of treatments (MM, MHT, and combination) after that, the cells were incubated for 24 h or 120 h in order to proceed with the cell viability assay or morphology analysis.

2.6. Cell Viability Assay

After treatments, the cells were transferred to 96-well plates in order to determine the cell viability assay. To evaluate cell viability, the MTT test (3-(4,5-dimethylthiazol-2-yl)-2,5-diphenyl tetrazolium bromide, Merck Bulgaria EAD 48 Sitnyakovo Blvd., Serdika Offices, 6th fl., Sofia 1505, Bulgaria) [24] was used. The absorbance was measured at 570 nm with plate reader (Tecan Infinite F200PRO, Tecan Austria GmbH, Salzburg). For each type of treatment, four replicates were used. The results were normalized to the control group (cells without MNPs and any treatment).

2.7. Cell Morphology Analysis

The changes in cell morphology were observed under microscope Axiovert 200 (Carl Zeiss, Jena, Germany) and 40 × objective at 24 h and 120 h after treatment. To evaluate the morphological changes in cells after treatments, ImageJ software (ImageJ, U. S. National Institutes of Health, Bethesda, MD, USA) was used to obtain cell shape parameters as a cell area and perimeter within an individual image and to calculate their circularity, roundness, aspect ratio (AR), and solidity as signs of morphological changes. To obtain those values cells from least five images for each treatment were analyzed.

Circularity can be calculated as a shape parameter index in the ImageJ software. The definition of circularity (CI) in the ImageJ software is as follows:

$$C_1 = 4\pi(A_1/P_1^2), \quad (1)$$

where A_1 and P_1 are the area and perimeter measured using ImageJ. When $C_1 = 1$, then the cell is circle.

The ImageJ software defines the aspect ratio as follows:

$$AR_1 = \text{major axis length of approximate ellipse} / \text{minor axis length of approximate ellipse} \quad (2)$$

Therefore, the aspect ratio is equal to one for a perfect circle and increases with an increase in deformation.

The roundness parameter (R) can be presented as follows:

$$R = 4 \times \text{Area} / (\pi \times \text{max diameter}^2) \quad (3)$$

When using R in particle shape analysis, the roundness values can be easily handled as numerical data.

Solidity is another cell parameter that ImageJ calculates as the area of a particle divided by its convex hull area:

$$S = \text{area} / \text{convex area} \quad (4)$$

2.8. Statistical Analysis

The data were analyzed using GraphPad Prism 5 (GraphPad Software, San Diego California USA) through one-way ANOVA and Tukey's post-hoc test. Student's t-test was used to determine if there is a significant difference between the different incubation times. The data were represented as mean \pm SD; the p value was represented as statistical significance and was set to $p < 0.05$.

3. Results and Discussion

3.1. Impact of Exposure of Cells to MH and MM

Figure 1 shows the hyperthermia temperature curves as a function of time for breast cancer (MCF-7) and non-cancerous (MCF-10A) cells, after magnetic hyperthermia (MHT), magneto-mechanical (MM) activation, and the combination of these two techniques (MHT and MM) with (w/) and without (w/o) MNPs. In all experiments, the magnetic field and the frequency were kept constant at 60 mT and 375 kHz, respectively. As it is obvious, in both cell lines, all samples with MNPs entered the hyperthermia window (41–45 °C), while the samples without MNPs did not (Figure 1a,b). The 41–45 °C temperature window is widely accepted as a regime able to lead cancer cells to apoptosis or even necrosis, depending on the phenotype features. In typical MHT setups, MHT is performed under non-adiabatic conditions, meaning that the samples under study are susceptible to temperature variations, due to heat exchanges with their surroundings. Therefore, the temperature increase that was observed in the samples (cancer or healthy cells) without MNPs is due to the heat transfer from the induction coil, but also due to the induced eddy currents, which are developed from the electric fields. These results are in agreement with relevant studies [26], where a similar temperature increase in the human monocytic leukemia cells (THP1) without MNPs, was also observed. The specific loss power (SLP), which is defined as the amount of induced heat per unit mass of MNPs per unit of time ($\Delta T / \Delta t$), was calculated in all samples containing healthy or cancer cells with MNPs. More specifically, the SLP value for cancer cells (MCF-7) after magnetic hyperthermia and after the combined treatment (magnetic hyperthermia and magneto-mechanical activation) was 1504 W/g. Accordingly, for the corresponding healthy cell line (MCF-10A) after magnetic hyperthermia and after the combined treatment (MHT and MM), the SLP value was 1170 W/g. These results are similar to those obtained by the research of Sakellari et al. [19], where the SLP values varied from 771 to 1044 W/g for 1 and 0.1 mg/mL, respectively. The concentration of MNPs

that we used in each under study sample was 0.1 mg/mL; therefore, this high SLP value, according to [19], is justified.

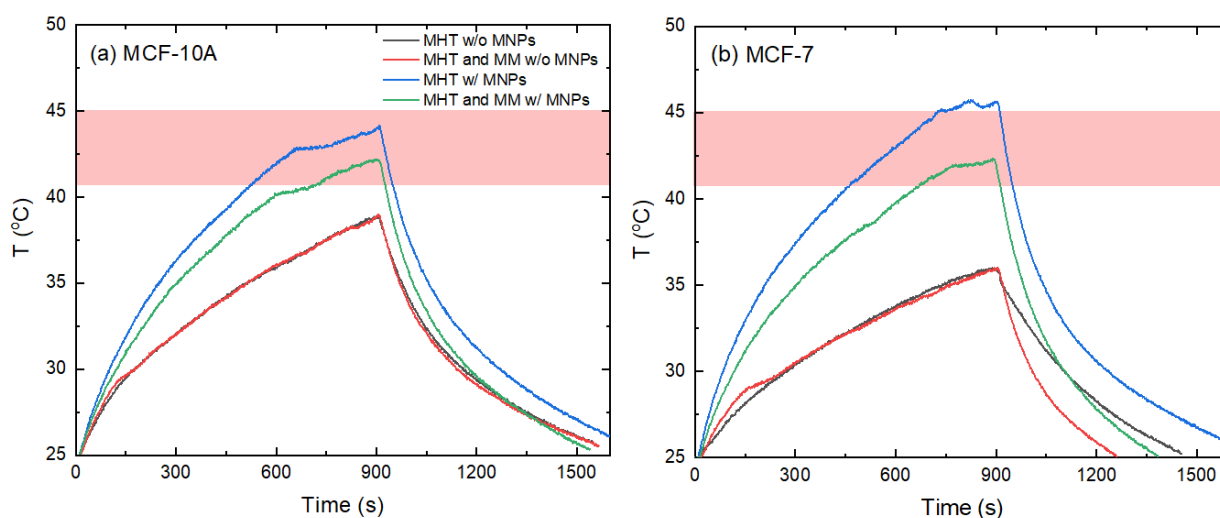


Figure 1. Experimental temperature against time curves for the (a) non-cancerous cell line (MCF-10A) and (b) cancer cell line (MCF-7) after magnetic hyperthermia (MHT), magneto-mechanical (MM) activation, and the combination of these two techniques (MHT and MM) with (w/) and without (w/o) MNPs. The applied experimental conditions were 60 mT/375 kHz. Shaded bands illustrate the hyperthermia window ($T = 41\text{--}45\text{ }^{\circ}\text{C}$).

3.2. Cell Viability

In our previous study, we established that pulsed field mode in presence of MNPs (Pulsed (+) MNPs) of MM activation caused the highest cytotoxic effect on breast cancer cells [18]. For that purpose, in the present study, we used that mode of MM activation in combination with MHT in order to check, if the combined treatment can induce an enhanced cytotoxic effect on breast cancer cells. The performed MTT assay showed excellent biocompatibility of MNPs in the used concentration as the cell viability was near to 100% for MCF-7 (Figure 2). For MCF-10A, the viability of MNPs after 120 h post-incubation was even above 100%, revealing good cell proliferation (Figure 3). This result is important because it shows that the MNPs themselves do not cause a toxic effect on the cells. In our previous work, we showed that MNPs at the same initial loading concentration of 100 $\mu\text{g}/\text{mL}$ were successfully internalized into cancer cells [18], and after 24 h of incubation they reached a concentration of 22,891 MNPs/cell, which proved to be toxic to cancer cells, when applying a low-frequency magnetic field [18]. The treatment of cancer cells (MCF-7) with MM (Pulsed (+) MNPs) revealed a long time (after 120 h incubation) effect on cell viability (under 50% decrease, as seen in Figure 2). In contrast, hyperthermia used alone did not have so strong an effect on cell viability. In Figure 2, it can be seen that cell viability kept values between 75 and 60% for both post-incubation periods. Apparently, after the application of combined treatment (MM and MHT), the cell viability dropped down very significantly to less than 20% (Figure 2), revealing the synergistic effect of combined treatment on cell viability.

MCF-10A cells treated with MM (pulsed (+) MNPs) or MHT (+ MNPs) separately showed lower survival rate at the shorter incubation time (24 h), while after 120 h post-incubation some recovery in cell viability was observed (Figure 3). Interestingly, the combined treatment (MM and MHT) of non-cancerous cells did not cause any enhanced effect on cell cytotoxicity. Probably, the higher sensitivity of MCF-10A to applied treatment (especially to MHT) is due to the easier and faster reaching of hyperthermic temperatures (Figure 1a).

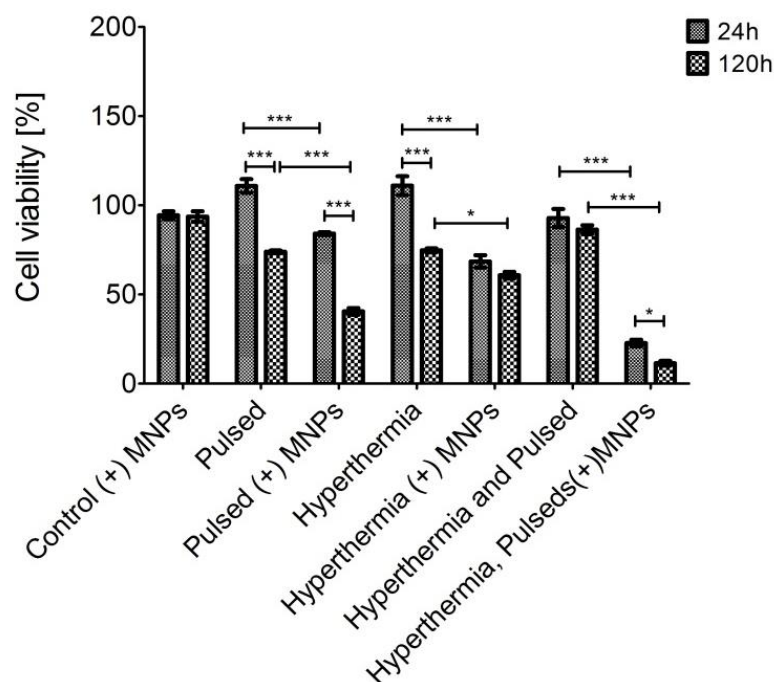


Figure 2. Cell viability of MCF-7 cells after series of treatments. Statistics was done by one-way ANOVA and Tukey's post-hoc test. The asterisks denote significant differences (*— $p < 0.05$ and ***— $p < 0.001$) between different treated cells as well as different incubation times.

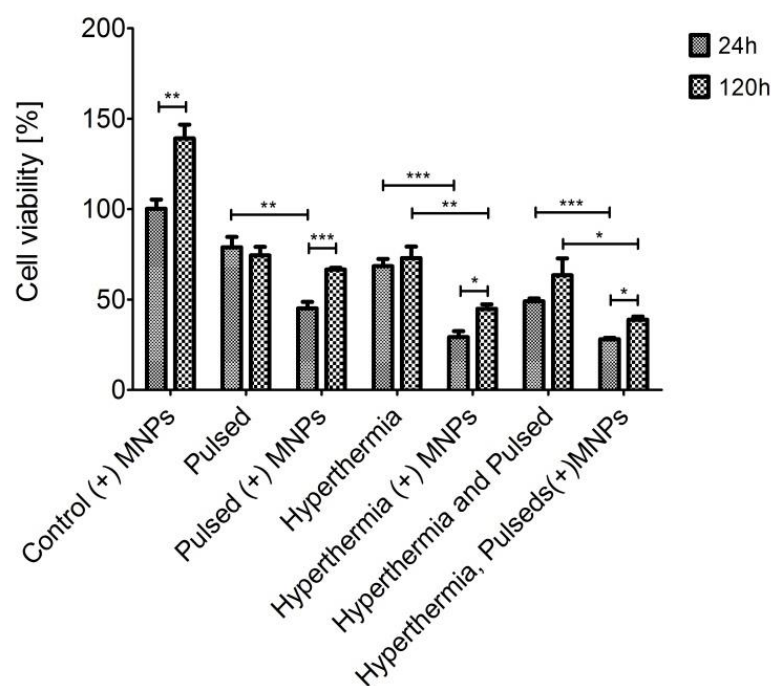


Figure 3. Cell viability of MCF-10A cells after series of treatments. Statistics was done by one-way ANOVA and Tukey's post-hoc test. The asterisks denote significant differences (*— $p < 0.05$, **— $p < 0.01$, ***— $p < 0.001$) between different treated cells as well as different incubation times.

3.3. Cell Morphology Assessment

The cell morphology of MCF-7 cells was examined by phase-contrast microscopy. Using the phase-contrast pictures and the ImageJ program, we calculated cell parameters as circularity, roundness aspect ratio, and solidity.

For the short post-incubation time (24 h, Figure 4 and Table 1), MCF-7 cells with almost all types of treatments showed more rounded cell morphology and enhanced solidity. AR levels were diminished, with the exception for cells treated with pulsed (+) MNPs and MHT without MNPs. The similar AR values of cells treated with pulsed (+) MNPs and MHT without MNPs to the value of the control confirmed the low effect of those treatments on cell viability shown earlier (Figure 4 and Table 1); 120 h after combined treatment the circularity of the cells became the highest (~1), which might be a consequence of the enhanced synergistic effect of this treatment on cell viability (Figure 5, Table 1). The roundness of MCF-7 treated in combination also retained the highest value (Table 1).

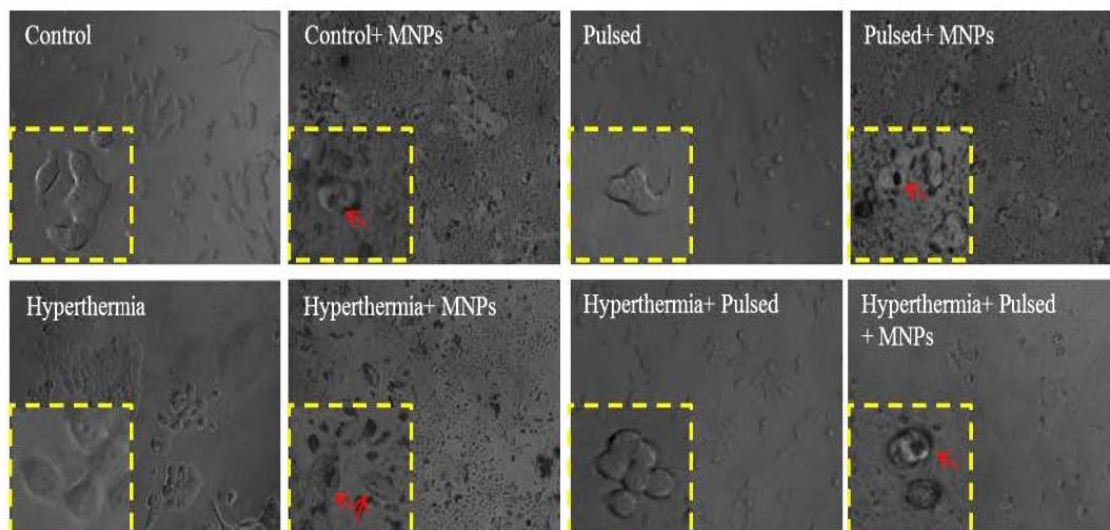


Figure 4. Phase-contrast images of MCF-7 after 24 h of different treatments. Yellow box—zoomed part of the image; red arrow—presence of MNPs in cells.

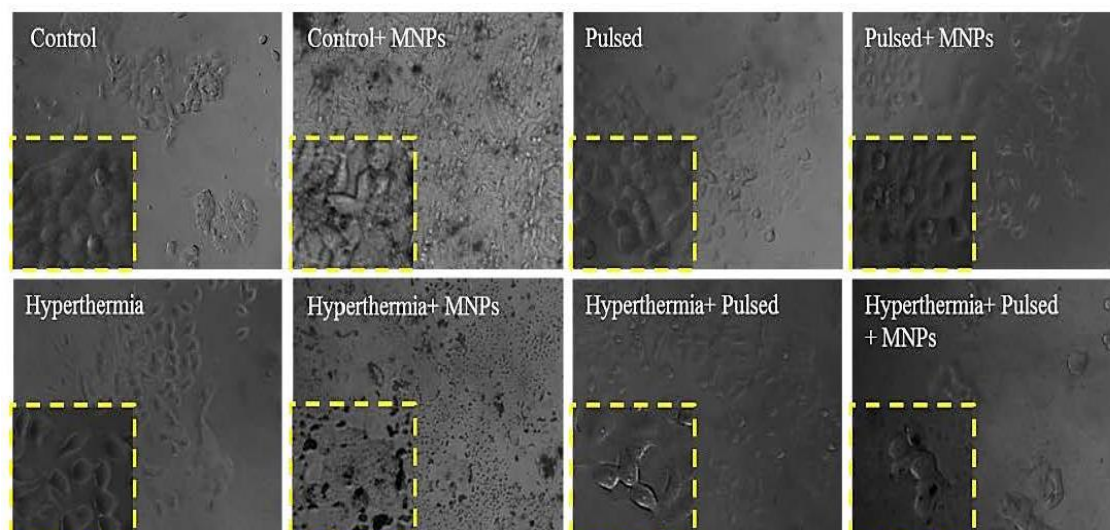


Figure 5. Phase-contrast images of MCF-7 after 120 h of different treatments. Yellow box—zoomed part of the image.

The typical MCF-10A cell morphology is elongated and spindle-shaped, indicated by a high AR coupled with low circularity (Figures 6 and 7, Table 2). When a combined treatment (MM and MHT) was applied to cells, their circularity increased (about ~ 0.75 at 24h) and their AR ratio decreased, respectively (Table 2). The solidity of the cells of combined treatment also showed the highest value (Table 2). The values of both parameters also remained the highest after 120 h for cells with combined treatment (Table 2).

Table 1. Circularity, roundness, AR, and solidity values calculated using Image J applied to the phase-contrast images of MCF-7 cells treated for 24 h and 120 h. Cells from at least five images for each treatment were analyzed. Statistics was done by one-way ANOVA and Tukey’s post-hoc test. All calculated values of different treatments were compared to the control. *— $p < 0.1$; **— $p < 0.01$; and ***— $p < 0.001$.

Type of treatment	Circularity		Roundness		AR (μm)		Solidity	
	24 h	120 h	24 h	120 h	24 h	120 h	24 h	120 h
Control	0.6	0.5	0.35	0.35	2.4	2.5	0.65	0.6
Control (+) MNPs	0.9 ***	0.6 **	0.5	0.5	1.5	1.8	0.8 ***	0.7
Pulsed	0.7 *	0.55	0.55	0.4	1.45 ***	2.2	0.7 **	0.7
Pulsed (+) MNPs	0.9 ***	0.6 *	0.45	0.45	2.5	2.4	0.9 ***	0.7
Hyperthermia	0.5 ***	0.7 ***	0.4	0.45	2.55	2.4	0.65	0.85 ***
Hyperthermia (+) MNPs	0.95 ***	0.8 ***	0.6 **	0.65 ***	1.92 ***	1.6*	0.9 ***	0.8 **
Hyperthermia and Pulsed	1 ***	0.8 ***	0.65 ***	0.45	1.4 ***	2.5	0.85 ***	0.75
Hyperthermia, pulsed (+) MNPs	1 ***	0.95 ***	0.58 **	0.7 ***	1.55 **	1.5 **	0.9 ***	0.8 ***

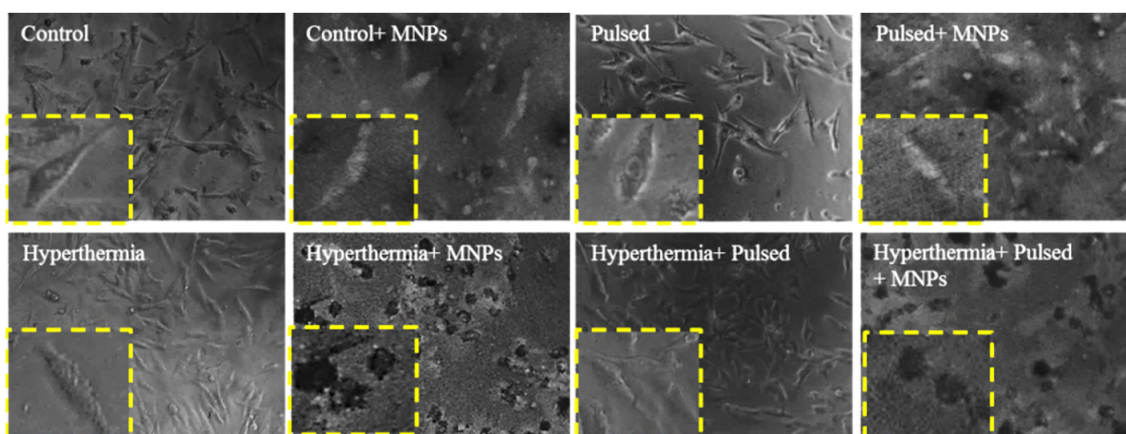


Figure 6. Phase-contrast images of MCF-10A after 24 h of different treatments. Yellow box—zoomed part of the image.

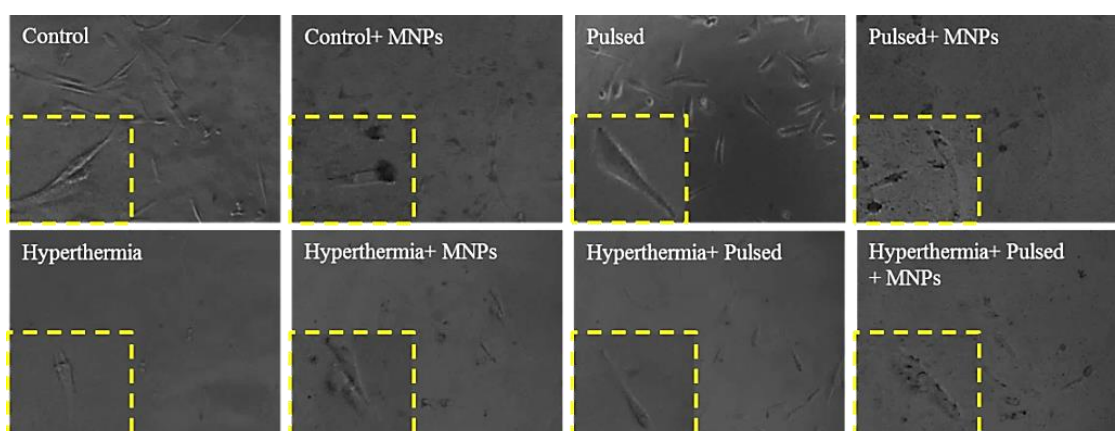


Figure 7. Phase-contrast images of MCF-10A after 120 h of different treatments. Yellow box—zoomed part of the image.

Table 2. Circularity, roundness, AR, and solidity values calculated using Image J applied to the phase-contrast images of MCF-10A cells treated for 24 h and 120 h. Cells from at least 5 images for each treatment were analyzed. Statistics was done by one-way ANOVA and Tukey’s post-hoc test. All calculated values of different treatments were compared to the control. *— $p < 0.1$; **— $p < 0.01$; and ***— $p < 0.001$.

Type of treatment	Circularity		Roundness		AR (μm)		Solidity	
	24 h	120 h	24 h	120 h	24 h	120 h	24 h	120 h
Control	0.3	0.2	0.4	0.35	1.9	2.2	0.55	0.5
Control (+) MNPs	0.45	0.25	0.7	0.4	1.5	1.5	0.6 ***	0.55
Pulsed	0.35	0.25	0.3	0.45	2.7	2	0.55 **	0.55
Pulsed (+) MNPs	0.6 ***	0.4 ***	0.45	0.37	2.2	2.4	0.7 ***	0.5
Hyperthermia	0.4 *	0.35 ***	0.5	0.5	2.4	1.8	0.55	0.55
Hyperthermia (+) MNPs	0.45 ***	0.4 ***	0.35	0.35	2	2.6	0.6 ***	0.53
Hyperthermia and pulsed	0.35 *	0.25 *	0.4	0.3	2.3	2.3	0.5 ***	0.5
Hyperthermia, pulsed (+) MNPs	0.75 ***	0.55 ***	0.55 *	0.55 *	1.6	1.7	0.8 ***	0.65 ***

It is worth mentioning that the application of MHT alone to MCF-7 did not cause visible apoptotic changes in the treated cells (Figure 8). Apoptotic changes were detected in MCF-7 cells treated with pulsed (+) MNPs alone and were more pronounced in cells with combined treatment (Figure 8). Obviously, the synergistic cytotoxic effect of the combined treatment also affects the process of apoptosis in cancer cells. Further research is needed to quantify this finding.

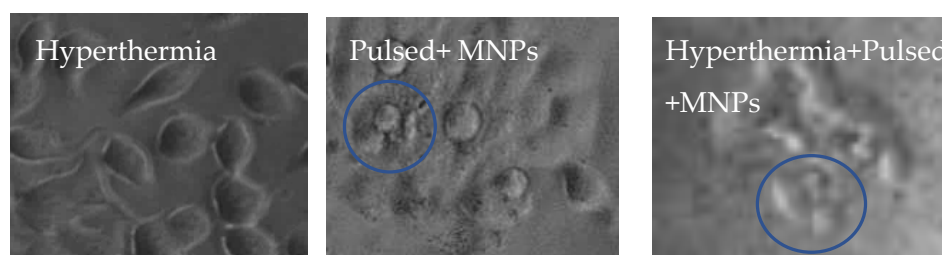


Figure 8. Apoptotic changes in MCF-7 cells after 120 h treatment. Circles denote apoptotic cells.

Previously published data from our group, others [18,24,27–29], and current data clearly show that magnetic nanoparticles transmit mechanical forces under an external magnetic field treatment, which can cause morphological alterations and cytoskeletal disruption, decreased cell viability, and subsequent cell death. In comparison, the application of MHT alone on cancer cells elicited milder cellular effects, which was shown by other authors [20], most probably because of the large thermal diffusivity in cells, and the impossibility of nanoparticles to produce significant localized heating to kill cells. However, when MHT was applied in combination with magneto-mechanical activation, an enhanced synergistic anticancer effect was observed.

4. Conclusions

In this work, the effect of combined magnetic hyperthermia and magneto-mechanical activation treatment on breast cancer cells (MCF-7) and non-cancer cells (MCF-10A) was studied. For MCF-7 cells, the combined treatment caused an enhanced synergistic effect on cell viability, circularity, and apoptosis, while for healthy MCF-10A cells such an enhanced effect of combined treatment was not observed.

From the above results, it can be concluded that by the combination of different types of treatments (MHT and MM), the therapeutic index of the cancer treatment can be

improved by having a synergistic therapeutic effect and a low effect on normal cells (low side effect).

Author Contributions: Conceptualization, R.T., M.A., T.S. (Theodoros Samaras) and O.K. formal analysis, V.U. and A.-R.T.; investigation, V.U. and A.-R.T.; methodology, V.U., A.-R.T. and T.S. (Tihomira Stoyanova), supervision, R.T., M.A., T.S. (Theodoros Samaras) and O.K.; validation, A.-R.T.; visualization, A.-R.T.; writing—original draft, V.U. and A.-R.T.; and writing—review and editing, R.T. All authors have read and agreed to the published version of the manuscript.

Funding: This work was supported by the Bulgarian Ministry of Education and Science under the National Research Program “Young scientists and postdoctoral students” approved by DCM#577/17.08.2018 and by Joint Research Project BAS-AUTH, 2018–2020.

Institutional Review Board Statement: Not applicable.

Informed Consent Statement: Not applicable.

Data Availability Statement: Not applicable.

Acknowledgments: The authors would like to acknowledge Antonios Makris from the Institute of Applied Biosciences—INAB in CERTH (Centre for Research and Technology Hellas) for the provision of laboratory equipment to carry out the experiments.

Conflicts of Interest: The authors declare no conflict of interest.

References

1. Hosu, O.; Tertis, M.; Cristea, C. Implication of Magnetic Nanoparticles in Cancer Detection, Screening and Treatment. *Magnetochemistry* **2019**, *5*, 55. [[CrossRef](#)]
2. Wang, H.; Qian, J.; Zhang, Y.; Xu, W.; Xiao, J.; Suo, A. Growth of MCF-7 breast cancer cells and efficacy of anti-angiogenic agents in a hydroxyethyl chitosan/glycidyl methacrylate hydrogel. *Cancer Cell Int.* **2017**, *17*, 55. [[CrossRef](#)] [[PubMed](#)]
3. Makridis, A.; Curto, S.; van Rhooon, G.C.; Samaras, T.; Angelakeris, M.A. standardisation protocol for accurate evaluation of specific loss power in magnetic hyperthermia. *J. Phys. D Appl. Phys.* **2019**, *52*, 255001. [[CrossRef](#)]
4. Wust, P.; Hildebrandt, B.; Sreenivasa, G.; Rau, B.; Gellermann, J.; Riess, H.; Felix, R.; Schlag, P.M. Hyperthermia in combined treatment of cancer. *Lancet Oncol.* **2002**, *3*, 487–497. [[CrossRef](#)]
5. Gordon, R.T.; Hines, J.R.; Gordon, D. Intracellular hyperthermia. A biophysical approach to cancer treatment via intracellular temperature and biophysical alterations. *Med. Hypotheses* **1979**, *5*, 83–102. [[CrossRef](#)]
6. Vilas-Boas, V.; Carvalho, F.; Espiña, B. Magnetic Hyperthermia for Cancer Treatment: Main Parameters Affecting the Outcome of In Vitro and In Vivo Studies. *Molecules* **2020**, *25*, 2874. [[CrossRef](#)]
7. Chang, D.; Lim, M.; Goos, J.A.C.M.; Qiao, R.; Ng, Y.Y.; Mansfeld, F.M.; Jackson, M.; Davis, T.P.; Kavallaris, M. Biologically Targeted Magnetic Hyperthermia: Potential and Limitations. *Front. Pharmacol.* **2018**, *9*, 831. [[CrossRef](#)]
8. Kirschning, A.; Kupracz, L.; Hartwig, J. New synthetic opportunities in miniaturized flow reactors with inductive heating. *Chem. Lett.* **2012**, *41*, 562–570. [[CrossRef](#)]
9. Kalamida, D.; Karagounis, I.V.; Mitrakas, A.; Kalamida, S.; Giatromanolaki, A.; Koukourakis, M.I. Fever-range hyperthermia vs. hypothermia effect on cancer cell viability, proliferation and HSP90 expression. *PLoS ONE* **2015**, *10*, e0116021. [[CrossRef](#)]
10. Gupta, R.; Sharma, D. Manganese-Doped Magnetic Nanoclusters for Hyperthermia and Photothermal Glioblastoma Therapy. *ACS Appl. Nano Mater.* **2020**, *3*, 2026–2037. [[CrossRef](#)]
11. Gupta, R.; Sharma, D. Evolution of Magnetic Hyperthermia for Glioblastoma Multiforme Therapy. *ACS Chem. Neurosci.* **2019**, *10*, 1157–1172. [[CrossRef](#)] [[PubMed](#)]
12. Luo, S.; Wang, L.F.; Ding, W.J.; Wang, H.; Zhou, J.M.; Jin, H.K.; Su, S.F.; Ouyang, W.W. Clinical trials of magnetic induction hyperthermia for treatment of tumours. *OA Cancer* **2014**, *18*, 2.
13. Maniotis, N.; Makridis, A.; Myrovali, E.; Theopoulos, A.; Samaras, T.; Angelakeris, M. Magneto-mechanical action of multimodal field configurations on magnetic nanoparticle environments. *J. Magn. Magn. Mater.* **2019**, *470*, 6–11. [[CrossRef](#)]
14. Cheng, Y.; Muroski, M.E.; Petit, D.C.M.C.; Mansell, R.; Vemulkar, T.; Morshed, R.A.; Han, Y.; Balyasnikova, I.V.; Horbinski, C.M.; Huang, X.; et al. Rotating magnetic field induced oscillation of magnetic particles for in vivo mechanical destruction of malignant glioma. *J. Control. Release* **2016**, *223*, 75–84. [[CrossRef](#)] [[PubMed](#)]
15. Spyridopoulou, K.; Makridis, A.; Maniotis, N.; Karypidou, N.; Myrovali, E.; Samaras, T.; Angelakeris, M.; Chlichlia, A.; Kalogirou. Effect of low frequency magnetic fields on the growth of MNP-treated HT29 colon cancer cells. *Nanotechnology* **2018**, *29*, 175101. [[CrossRef](#)]
16. Zhang, E.; Kircher, M.F.; Koch, M.; Eliasson, L.; Goldberg, S.N.; Renström, E. Dynamic magnetic fields remote-control apoptosis via nanoparticle rotation. *ACS Nano* **2014**, *8*, 192–201. [[CrossRef](#)]

17. Leulmi, S.; Chauchet, X.; Morcrette, M.; Ortiz, G.; Joisten, H.; Sabon, P.; Livache, T.; Hou, Y.; Carrière, M.; Lequien, S.; et al. Triggering the apoptosis of targeted human renal cancer cells by the vibration of anisotropic magnetic particles attached to the cell membrane. *Nanoscale* **2015**, *7*, 15904–15914. [[CrossRef](#)] [[PubMed](#)]
18. Tsiapla, A.R.; Uzunova, V.; Oreshkova, T.; Angelakeris, M.; Samaras, T.; Kalogirou, O.; Tzoneva, R. Cell Behavioral Changes after the Application of Magneto-Mechanical Activation to Normal and Cancer Cells. *Magnetochemistry* **2022**, *8*, 21. [[CrossRef](#)]
19. Sakellari, D.; Mathioudaki, S.; Kalpaxidou, Z.; Simeonidis, K.; Angelakeris, M. Exploring multifunctional potential of commercial ferrofluids by magnetic particle hyperthermia. *J. Magn. Magn. Mater.* **2015**, *380*, 360–364. [[CrossRef](#)]
20. Giustini, A.J.; Petryk, A.A.; Cassim, S.M.; Tate, J.A.; Baker, I.; Hoopes, P.J. Magnetic Nanoparticle Hyperthermia in Cancer Treatment. *Nano Life* **2010**, *1*, 17–32. [[CrossRef](#)]
21. Zamora-Mora, V.; Fernández-Gutiérrez, M.; González-Gómez, Á.; Sanz, B.; San Román, J.; Goya, G.F.; Mijangos, C. Chitosan nanoparticles for combined drug delivery and magnetic hyperthermia: From preparation to in vitro studies. *Carbohydr. Polym.* **2017**, *157*, 361–370. [[CrossRef](#)] [[PubMed](#)]
22. De Paula, L.B.; Primo, F.L.; Pinto, M.R.; Morais, P.C.; Tedesco, A.C. Evaluation of a chloroaluminium phthalocyanine-loaded magnetic nanoemulsion as a drug delivery device to treat glioblastoma using hyperthermia and photodynamic therapy. *RSC Adv.* **2017**, *7*, 9115–9122. [[CrossRef](#)]
23. Angelakeris, M.; Li, Z.A.; Sakellari, D.; Simeonidis, K.; Spasova, M.; Farle, M. Can commercial ferrofluids be exploited in AC magnetic hyperthermia treatment to address diverse biomedical aspects? *EDP Sci. EPJ Web Conf.* **2014**, *75*, 08002. [[CrossRef](#)]
24. Uzunova, V.; Tsiapla, A.R.; Stoyanova, T.; Myrovali, E.; Momchilova, A.; Kalogirou, O.; Tzoneva, R. Biocompatibility of iron oxide nanoparticles. *J. Chem. Technol. Metall.* **2021**, *56*, 1187–1191.
25. Tsiapla, A.R.; Kalimeri, A.A.; Maniotis, N.; Myrovali, E.; Samaras, T.; Angelakeris, M.; Kalogirou, O. Mitigation of magnetic particle hyperthermia side effects by magnetic field controls. *Int. J. Hyperth.* **2021**, *38*, 511–522. [[CrossRef](#)] [[PubMed](#)]
26. Carrasco, D.C. Addressing the Dynamical Magnetic Response of Magnetic Nanoparticles after Interacting with Biological Entities. Doctoral Dissertation, Universidad Autónoma de Madrid, Madrid, Spain, 2018.
27. Golovin, Y.I.; Gribovsky, S.L.; Golovin, D.Y.; Klyachko, N.L.; Majouga, A.G.; Master, A.M.; Sokolsky, M.; Kabanov, A.V. Towards nanomedicines of the future: Remote magneto-mechanical actuation of nanomedicines by alternating magnetic fields. *J. Control. Release* **2015**, *219*, 43–60. [[CrossRef](#)]
28. Master, A.M.; Williams, P.N.; Pothayee, N.; Pothayee, N.; Zhang, R.; Vishwasrao, H.M.; Golovin, Y.I.; Riffle, J.S.; Sokolsky, M.; Kabanov, A.V. Remote actuation of magnetic nanoparticles for cancer cell selective treatment through cytoskeletal disruption. *Sci. Rep.* **2016**, *6*, 33560. [[CrossRef](#)]
29. Wong, W.; Gan, W.L.; Teo, Y.K.; Lew, W.S. Interplay of cell death signaling pathways mediated by alternating magnetic field gradient. *Cell Death Discov.* **2018**, *4*, 49. [[CrossRef](#)]